

Unsupervised Segmentation Using Gabor Wavelets and Statistical Features in LIDAR Data Analysis

Hong Wei and Marc Bartels
School of Systems Engineering
The University of Reading
Reading RG6 6AY, UK
[h.wei, m.bartels]@reading.ac.uk
<http://www.cvg.rdg.ac.uk/projects/LIDAR/>

Abstract

In this paper, we address issues in segmentation of remotely sensed LIDAR (LIght Detection And Ranging) data. The LIDAR data, which were captured by airborne laser scanner, contain 2.5 dimensional (2.5D) terrain surface height information, e.g. houses, vegetation, flat field, river, basin, etc. Our aim in this paper is to segment ground (flat field) from non-ground (houses and high vegetation) in hilly urban areas. By projecting the 2.5D data onto a surface, we obtain a texture map as a grey-level image. Based on the image, Gabor wavelet filters are applied to generate Gabor wavelet features. These features are then grouped into various windows. Among these windows, a combination of their first and second order of statistics is used as a measure to determine the surface properties. The test results have shown that ground areas can successfully be segmented from LIDAR data. Most buildings and high vegetation can be detected. In addition, Gabor wavelet transform can partially remove hill or slope effects in the original data by tuning Gabor parameters.

1. Introduction

Airborne laser scanned LIDAR data have become popular in remote sensing, land surveying and mapping for the last decade [1]. The reflected laser pulses form the Earth surface model, named Digital Surface Model (DSM) as 2.5D data. The interpolated LIDAR tiles (as a matrix) register with the Global Positioning System (GPS) to provide detailed surface information, e.g. buildings, vegetation, rivers, basins, etc. The development of LIDAR sensors has achieved the high resolution of 0.25m in horizontal, and accuracy of 5-20 cm in vertical directions [2]. Compared to the LIDAR sensor technology, LIDAR post-processing becomes as a bottle-neck to put the technology in real uses [3]. This

places a demand for development of algorithms which can automatically interpret LIDAR data. In some applications, for example, flood modelling, the bare-Earth model, called Digital Terrain Model (DTM) is required [4]. From the DSM to DTM, the first step is to remove buildings and high vegetation from the original LIDAR data. The existing algorithms for this purpose in the remote sensing community are still limited and not reliable [3]. Our work in this paper aims to segment ground areas (flat field) from non-ground, e.g. buildings and high vegetation (trees and bushes). The methodology that we proposed is to project the 2.5D LIDAR data onto a surface in order to exploit texture analysis techniques established in image processing.

Gabor filters have been used widely in image texture analysis due to their nature of spatial locality, orientation selectivity, and frequency characteristic [5, 6]. Gabor wavelets model the receptive field profiles of cortical simple cells [7], and they are optimally localised in the space and frequency domain [8]. Gabor wavelet representation captures salient visual properties, e.g. discontinuity in gradient. It is popular in the pattern recognition and image processing communities for texture segmentation. Dunn, *et. al.* declared that distinct discontinuities occur only if the Gabor filter parameters are suitably chosen [9]. They then devised a rigorously based method for designing Gabor filters in texture segmentation. Kyrki, *et. al.* worked in a simple Gabor feature space for invariant object recognition [10]. Randen, *et. al.* suggested in [11] that the Gabor filter bank might be good in texture segmentation for different types of texture images based on scale, orientation, and frequency tuning.

We apply Gabor wavelets to airborne laser scanned LIDAR data to generate their Gabor wavelet representation, which is then grouped into small windows as segmentation units. Thus, the first and second order of statistics of these windows, such as mean and standard deviation, are used as measures to

segment ground and non-ground areas. The paper is organised as follows. In Section 2, Gabor wavelet representation is presented. Section 3 discusses the statistical measures, and how to use these measures to determine terrain properties. We demonstrate the test results in Section 4 with relevant discussions. The paper concludes and points out limits for further investigations in Section 5.

2. Gabor wavelet representation

In the spatial domain, 2D Gabor wavelets can be expressed by a Gaussian kernel modulated by a complex plane wave [6].

$$g_{\mu,\nu}(x,y) = \frac{\|k_{\mu,\nu}\|^2}{2\pi\sigma^2} e^{-\frac{\|k_{\mu,\nu}\|^2(x^2+y^2)}{2\sigma^2}} [e^{ik_{\mu,\nu}(x+y)} - e^{-\frac{\sigma^2}{2}}] \quad (1)$$

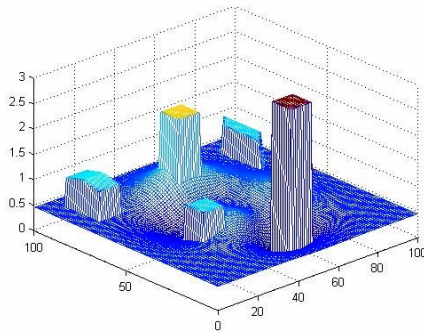
where $k_{\mu,\nu}$ is the wave vector defined by both orientation μ and scale ν , and is constructed as

$$k_{\mu,\nu} = k_\nu e^{i\phi_\mu} \quad (2)$$

In Equation (1), the first term in the square bracket is the oscillatory part in the Gabor kernel, and the second term contributes to the property of DC free. The parameter σ determines the ratio of the Gaussian window width and wavelength. In Equation (2),

$$k_\nu = \frac{k_{\max}}{f^\nu} \text{ and } \phi_\mu = \frac{\pi\nu}{4}. \text{ In our experiments, we use}$$

$$k_{\max} = \frac{\pi}{2}, \text{ which is the Nyquist frequency, and } f = \sqrt{2},$$



(a) Artificial ground with house blocks

which is the spacing factor between kernels in the frequency domain. In the test, three scales and four orientations of Gabor wavelets were used as $\nu \in \{0,1,2\}$ and $\mu \in \{0,1,2,3\}$. Figure 1 shows the real part of these Gabor kernels and their magnitude, with $\sigma = 2\pi$.

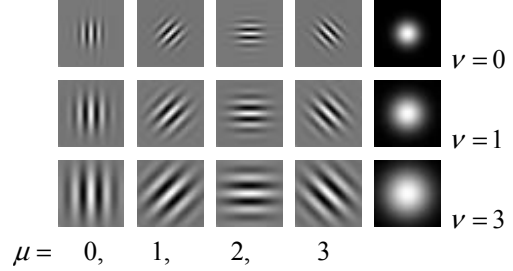


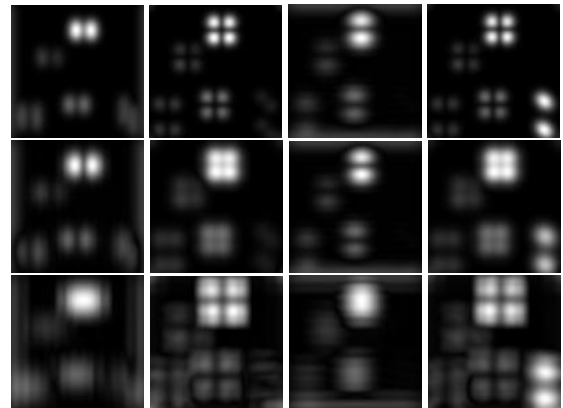
Figure 1. Gabor wavelets

Gabor wavelet representation of the projected LIDAR data $d(x,y)$ is defined as

$$r_{\mu,\nu}(x,y) = d(x,y) * g_{\mu,\nu}(x,y) \quad (3)$$

where $*$ denotes the convolution operator in the spatial domain, and $r_{\mu,\nu}(x,y)$ is the Gabor wavelet representation corresponding to the kernel at orientation μ and scale ν . It has its complex structure with real part $\Re\{r_{\mu,\nu}(x,y)\}$ and imaginary part $\Im\{r_{\mu,\nu}(x,y)\}$. We use its magnitude as the response, which can be written as

$$\|r_{\mu,\nu}(x,y)\| = \sqrt{\Re^2\{r_{\mu,\nu}(x,y)\} + \Im^2\{r_{\mu,\nu}(x,y)\}} \quad (4)$$



(b) Gabor wavelet representations (the order corresponding to that in Figure 1)

Figure 2. Artificial DSM mesh (a) and its Gabor wavelet representations (b)

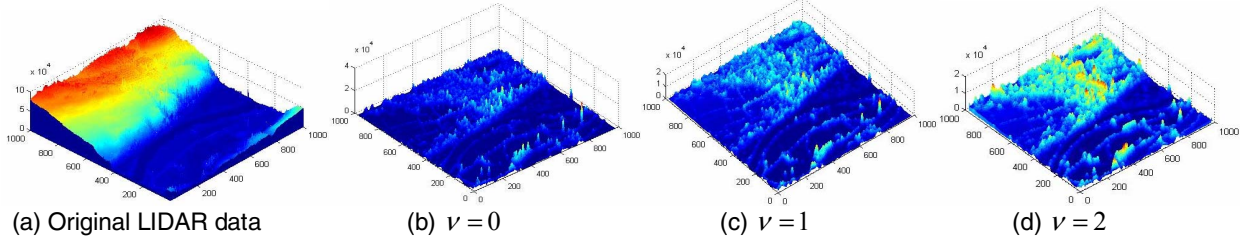


Figure 3. LIDAR data (Copyright © Environment Agency) and its Gabor wavelet representation in three scales

Figure 2 demonstrates an artificial DSM and its Gabor wavelet representations. Figure 2(a) is the 3D mesh of the DSM with house blocks of different shapes on it. The artificial ground is a wave plane. By applying the Gabor wavelets in Figure 1 to the artificial data, we obtain its Gabor wavelet representations as shown in Figure 2(b). It can be clearly seen that Gabor features in Figure 2(b) reflect local discontinuities with orientation selectivity. Considering the characteristic of orientation selectivity, we mixed all Gabor features in the same scale to generate the mixture of the representation as

$$r^v(x, y) = \sum_{\mu=0}^3 \omega_{\mu} \|r_{\mu, v}(x, y)\| \quad (5)$$

where ω_{μ} is a weight assigned to each orientation responses, and satisfies $\sum_{\mu=0}^3 \omega_{\mu} = 1$.

In Figure 3, a mesh of a LIDAR data tile and its Gabor wavelet representations are presented. From Figure 3(a), we can see the challenging slope in the original data. Figures 3(b), 3(c) and 3(d) demonstrate the mixture of Gabor wavelet representation of the original LIDAR data in scales of $\nu=0$, $\nu=1$, and $\nu=2$, respectively. The observation from the experimental analysis indicates that the Gabor wavelet representation with $\nu=0$ removes the slope entirely, while the others can only partially remove the slope. This means that it is important to tune the scale in real applications for the purpose of slope removal.

3. Statistical measures

The Gabor wavelet representation captures responses of local discontinuities. For flat fields, it is assumed that the responses are very low. For residential areas with houses and high vegetation, the responses are relatively high. Based on this fact, we sub-divide the Gabor wavelet representation into small windows with size of $m \times n$. Then we calculate their first and second order of

statistics, *i.e.* mean and standard deviation as defined in Equations (6) and (7), respectively.

$$mean_w = \frac{1}{m \times n} \sum_{i=1}^m \sum_{j=1}^n r^v(x_i, y_j) \quad (6)$$

$$std_dev_w = \sqrt{\frac{\sum_{i=1}^m \sum_{j=1}^n [r^v(x_i, y_j) - mean_w]^2}{m \times n - 1}} \quad (7)$$

where $w \in \{1, 2, \dots, N\}$ represents the number of windows used in segmentation.

Table 1 shows the segmentation results based on the measures in Equations (6) and (7). A window area is segmented as flat field if its mean is low, while it is recognised as non-ground if the mean is high and the standard deviation is low. In Table 1, there are so-called grey areas, where the std_dev_w has relatively high values when the mean shows high responses. For this type of areas, the segmentation stands for *non-ground*. However, further investigation is needed when ground-truth becomes available. This observation is also discussed in Section 4 with test results.

Table 1. Segmentation decision vs measures

		$mean_w$	
		Low	High
std_dev_w	Low	Flat field	Buildings and high vegetation
	High	Flat field	Grey areas

4. Test results and discussions

LIDAR data we used in the test were supplied by the UK Environment Agency (EA). LIDAR data tiles were processed by using the developed algorithm. The validation was carried out by using related optical data which were also provided by the EA. Figure 4 demonstrates the optical data and the segmentation results of two tiles. Figures 4(b) and 4(d) clearly demonstrate that flat fields were accurately segmented

without effects of slope which was appeared in the original LIDAR data. We treated this type of areas as *ground*. For the grey areas, we observed from Figure 4(b) that they most likely represented bushes in the data. This can be proved in Figure 4(d) where there were less grey areas because of few bushes in the original data.

The segmentation results were generated by using Gabor wavelet representation in the scale of $\nu = 0$. The reason is that it provided better solutions for slope removal. The test tiles used in our experiments all contain hilly urban areas. In the experimental analysis, it was also observed that the kernel frequency controlled by the value of σ affects the responses of Gabor wavelets. For Tile 2, the Gabor wavelets were generated by tuning $\sigma = \pi$. Otherwise, the slope existing in the original data would not be removed.

Investigation brought a problem up to the surface, *i.e.* large flat roof buildings may also be classified as a flat field. This is because there is continuous gradient in the area of the roof. In this case, other methods, *e.g.* morphologic filtering, etc. may be employed for processing. The elevation information from the original data can also be used for local height estimation. We leave this data fusion problem for the future research.

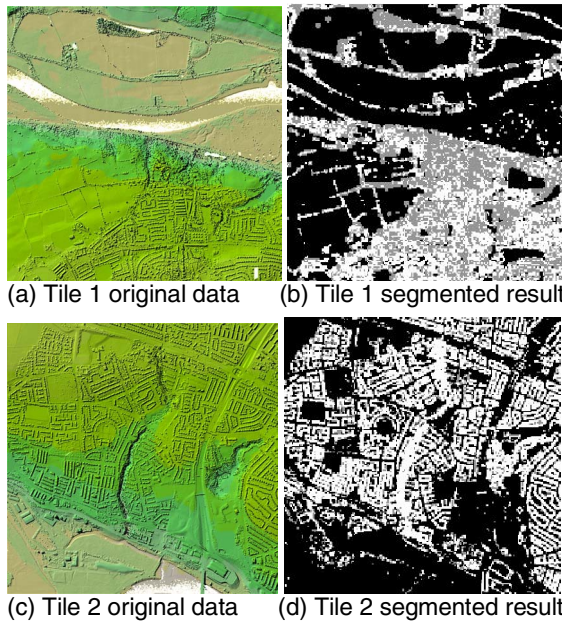


Figure 4. Test results

5. Conclusions

We developed an algorithm aiming to segment ground (*e.g.* buildings and high vegetation) and non-ground (flat fields) in airborne scanned LIDAR data. This is the very first step for terrain feature classification

based on LIDAR data. The developed algorithm can segment flat fields accurately with very low false negative. It is important in real applications to exclude this type of data to reduce computation expenses. Certainly we still need to face the false positive problem as the flat roof of large buildings. Those data segmented as non-ground will be used in the further study of terrain feature classification. In that stage, other techniques, such as data fusion will be introduced.

6. Acknowledgement

We would like to thank the UK Environment Agency for supplying LIDAR data. The project is partially funded by RETF of the University of Reading.

7. References

- [1] H. G. Maas, Akquisition von 3D-GIS Daten durch Flugzeuglaserscanning, *Kartographische Nachrichten*, 55(1), 2005, pp. 3-11
- [2] E. J. Huising and L. M. Gomes Pereira, "Errors and Accuracy Estimates of Laser Data Acquired by Various Laser Scanning Systems for Topographic Applications", *ISPRS Journal of Photogrammetry & Remote Sensing*, vol. 53, 1998, pp. 245-261
- [3] T. T. Vu, M. Matsuoka, and F. Yanmazaki, "LIDAR Signatures to Update Japanese Building Inventory Databas", *Asian Conference of Remote Sensing*, Chianmai, Thailand, November 2004, pp. 624-629
- [4] S. J. Maybank, R. V. Fraile, V. Prinnet, F. Wang, Z. H. Zhang, and G. Wu, "Scene Modeling from Remote Sensing Data", *Workshop on Information Technologies for Flood Management*, Beijing, 17 Sept. 2001
- [5] Anil K. Jain and Farshid Farrokhnia, "Unsupervised Texture Segmentation Using Gabor Filters", *Pattern Recognition*, vol. 24, no. 12, 1991, pp. 1167-1185
- [6] Chengjun Liu, "Gabor-based Kernel PCA with Fractional Power Polynomial Models for Face Recognition", *IEEE Transaction on Pattern Analysis and Machine Intelligence*, vol.26, no.5, 2004, pp. 572-581
- [7] J. G. Daugman, "Two-Dimension Spectral Analysis of Cortical Receptive Field Profiles", *Vision Research*, vol. 20, 1980, pp. 847-856
- [8] Tai Sing Lee, "Image Representation Using 2D Gabor Wavelets", *IEEE Transaction on Pattern Analysis and Machine Intelligence*, vol.18, no.10, 1996, pp. 959-971
- [9] D. Dunn and W. E. Higgins, "Optimal Gabor filters for Texture Segmentation", *IEEE Transaction on Image Processing*, vol. 4, no. 7, 1995, pp. 947-964
- [10] V. Kyrki, J. K. Kamarainen, and H. Kalviainen, "Simple Gabor Feature Space for Invariant Object Recognition", *Pattern Recognition Letters*, vol.25, no. 3, 2004, pp. 311-318
- [11] T. Randen and J. H. Husoy, "Filtering for Texture Classification: A Comparative Study", *IEEE Transaction on Pattern Analysis and Machine Intelligence*, vol. 21, no. 4, 1999, pp. 291-31